World Journal of Microbiology and Biotechnology (2024) 40:219
https://doi.org/10.1007/s11274-024-04032-9

RESEARCH

Biotransformation of docosahexaenoic acid into 10*R*,17*S*-dihydroxydocosahexaenoic acid as protectin DX 10-epimer by serial reactions of arachidonate 8*R*- and 15*S*-lipoxygenases

Tae-Eui Lee[1] · Yoon-Joo Ko[2] · Kyung-Chul Shin[3] · Deok-Kun Oh[1]

Received: 14 November 2023 / Accepted: 22 May 2024 / Published online: 29 May 2024

Abstract

Protectins, 10,17-dihydroxydocosahexaenoic acids (10,17-DiHDHAs), are belonged to specialized pro-resolving mediators (SPMs). Protectins are generated by polymorphonuclear leukocytes in humans and resolve inflammation and infection in trace amounts. However, the quantitative production of protectin DX 10-epimer (10-epi-PDX, 10*R*,17*S*-4*Z*,7*Z*,11*E*,13*Z*,15*E*,19*Z*-DiHDHA) has been not attempted to date. In this study, 10-epi-PDX was quantitatively produced from docosahexaenoic acid (DHA) by serial whole-cell biotransformation of *Escherichia coli* expressing arachidonate (ARA) 8*R*-lipoxygenase (8*R*-LOX) from the coral *Plexaura homomalla* and *E. coli* expressing ARA 15*S*-LOX from the bacterium *Archangium violaceum*. The optimal bioconversion conditions to produce 10*R*-hydroxydocosahexaenoic acid (10*R*-HDHA) and 10-epi-PDX were pH 8.0, 30 °C, 2.0 mM DHA, and 4.0 g/L cells; and pH 8.5, 20 °C, 1.4 mM 10*R*-HDHA, and 1.0 g/L cells, respectively. Under these optimized conditions, 2.0 mM (657 mg/L) DHA was converted into 1.2 mM (433 mg/L) 10-epi-PDX via 1.4 mM (482 mg/L) 10*R*-HDHA by the serial whole-cell biotransformation within 90 min, with a molar conversion of 60% and volumetric productivity of 0.8 mM/h (288 mg/L/h). To the best of our knowledge, this is the first quantitative production of 10-epi-PDX. Our results contribute to the efficient biocatalytic synthesis of SPMs.

Key points

Protectin DX 10-epimer was produced from docosahexaenoic acid by 8*R*- and 15*S*-lipoxygenases.
The reaction conditions for the production of protectin DX 10-epimer were optimized.
This is an efficient, cost-effective, and eco-friendly production of protectin DX 10-epimer.

Keywords Arachidonate 8*R*-lipoxygenase · Arachidonate 15*S*-lipoxygenase · 10*R*,17*S*-dihydroxydocosahexaenoic acid · Protectin DX 10-epimer · Specialized pro-resolving mediator

✉ Kyung-Chul Shin
kcshin@hufs.ac.kr

✉ Deok-Kun Oh
deokkun@konkuk.ac.kr

Tae-Eui Lee
legals1@naver.com

Yoon-Joo Ko
yjko@snu.ac.kr

[1] Department of Bioscience and Biotechnology, Konkuk University, Seoul 05029, Republic of Korea

[2] National Center for Inter-University Research facilities (NCIRF), Seoul National University, Seoul 08826, Republic of Korea

[3] Department of Bioscience and Biotechnology, Hankuk University of Foreign Studies, Yongin 17035, Republic of Korea

Introduction

Specialized pro-resolving mediators (SPMs) are C20 and C22 dihydroxy and trihydroxy fatty acids and are generated in trace amounts from polyunsaturated fatty acids (PUFAs), including arachidonic acid (ARA), eicosapentaenoic acid (EPA), docosapentaenoic acid (DPA), and docosahexaenoic acid (DHA), by the transcellular reactions of M2 macrophages or polymorphonuclear leukocytes (PMNs) in humans via the combined biosynthesis of regioselective lipoxygenases (LOXs), cyclooxygenase, and cytochrome P450 (An et al. 2021). SPMs have attracted great attention as leading compounds in treatment of inflammation and infection in trace amounts (Morita et al. 2013; Serhan et al. 2015a; Weylandt 2016). Among the SPMs, lipoxins have anti-obesity activity (Borgeson et al. 2015), resolvins (Rvs) have sepsis control (Spite et al. 2009) and tissue protection activities (Gobbetti et al. 2017), maresins (MaRs) have tissue regeneration activity (Serhan et al. 2009), and protectins have anti-apoptotic (Antony et al. 2010), neuroprotective (Asatryan and Bazan 2017), anti-oxidant (Hwang et al. 2019), and anti-viral activities (Lagarde et al. 2020; Morita et al. 2013).

The synthesis of SPMs by mammalian cell culture is not viable because they are produced in small amounts (10 − 500 ng/L) (Werz et al. 2018). Furthermore, purified mammalian LOXs produce SPMs at very low concentrations (< 40 μM) (Perry et al. 2020). Thus, SPMs have so far been synthesized by chemical methods. However, the methods are expensive and environmentally unfriendly because of the many (20 − 30) step reactions, low yields (< 30%), and pollution from heavy metals, such as $Pd(PPh_3)_4$ and $CrCl_2$, and harmful materials, such as benzene and tetrahydrofuran (Dayaker et al. 2014; Rodriguez and Spur 2005; Sanceau et al. 2019; Tungen et al. 2015).

To overcome these problems, bacterial double-oxygenating LOXs have been recently suggested as efficient SPM and SPM isomer producers. For instance, bacterial double-oxygenating ARA 9*S*-, 12*S*-, and 15*S*-LOXs convert PUFAs into 170 − 2120 mg/L of SPM and SPM isomers, including 11*S*,17*S*-dihydroxydocosahexaenoic acid (11*S*,17*S*-DiHDHA) and 11*S*,17*S*-dihydroxydocosapentaenoic acid (11*S*,17*S*-DiHDPA) as protectin DX 11-isomer (11*S*,17*S*-DiHDHA) and PDX_{n-3} 11-isomer (11*S*,17*S*-DiHDPA) (Oh et al. 2022), 7*S*,14*S*-DiHDHA and 7*S*,14*S*-DiHDPA as the 10-*cis*-12-*trans*-7*S*-epimers of maresin 1 (MaR1) (7*R*,14*S*-DiHDHA) and $MaR1_{n-3}$ (7*R*,14*S*-DiHDPA) (Kim et al. 2021), and resolvin E4 (RvE4, 5*S*,15*S*-dihydroxyeicosapentaenoic acid, 5*S*,15*S*-DiHEPA), resolvin D5 (RvD5, 7*S*,17*S*-DiHDHA), and $RvD5_{n-3}$ (7*S*,17*S*-DiHDPA) (Lee et al. 2020), respectively. In contrast, the SPM PDX is synthesized by the combined reactions of 8*S*- and 15*S*-LOXs (Shin et al. 2022) because mouse double-oxygenating 8*S*-LOX, the only reported 8*S*-LOX, shows 310 − 680-fold lower activity in the second oxygenation than the bacterial double-oxygenating LOXs (Kim et al. 2021; Lee et al. 2020; Oh et al. 2022). Protectin DX 10-epimer (10-epi-PDX, 10*R*,17*S*-DiHDHA) can only be produced by the combined reactions of single-oxygenating 8*R*- and 15*S*-LOXs because there are no double-oxygenating LOXs that perform both *R*- and *S*-form oxygenation.

Protectin D1 (PD1, 10*R*,17*S*-4*Z*,7*Z*,*11E*,*13E*,*15Z*,19*Z*-DiHDHA), protectin D1 10-epimer (10-epi PD1, 10*S*,17*S*-4*Z*,7*Z*,*11E*,*13E*,*15Z*,19*Z*-DiHDHA), PDX (10*S*,17*S*-4*Z*,7*Z*,*11E*,*13Z*,*15E*,19*Z*-DiHDHA), and 10-epi-PDX (10*R*,17*S*-4*Z*,7*Z*,*11E*,*13Z*,*15E*,19*Z*-DiHDHA) are 10,17-DiHDHAs with different stereoselectivity and *E*-*Z* isomerism (Fig. 1). In addition, 10,17-DiHDHAs have several isomers for protectin D1, including 10-epi-*S*-15-Δ-*trans* of PD1 and 15-Δ-*trans* of PD1 and PD2 (Stenvik Haatveit and Hansen 2023). Among protectins, 10-epi-PDX was found as protectin isomer IV, and it exhibits an anti-inflammatory effect equivalent to that of PDX (Serhan et al. 2006). This protectin is generated in trace amounts by PMNs in humans (Serhan et al. 2006) and it is also detected in the conversion of 10-hydroxydocosahexaenoic acid (10-HDHA) by soybean 15*S*-LOX (Chen et al. 2009). However, the quantitative production of 10-epi-PDX has not been attempted to date. To provide enough amounts of the pure substance for research purposes, the study on the quantitative production of 10-epi-PDX is needed.

In this study, a serial whole-cell biotransformation was developed to quantitatively produce 10-epi-PDX from DHA via 10*R*-HDHA. In the biotransformation, *Escherichia coli* expressing 8*R*-LOX from the coral *Plexaura homomalla* first converted DHA into 10*R*-HDHA, which was then converted into 10-epi-PDX by *E. coli* expressing 15*S*-LOX from the bacterium *Archangium violaceum*.

Materials and methods

Materials

DHA standard was purchased from Sigma-Aldrich (St. Louis, MO, USA). 10*S*-HDHA, 10(±)-HDHA, 17*S*-HDHA, PDX, and RvD5 standards were purchased from Cayman Chemical (Ann Arbor, MI, USA). 16,17-Hepoxilin B_5 (15*R*-hydroxy-16*S*,17*S*-epoxy-docosahexaenoic acid) was prepared as previously reported (Lee et al. 2019). 10*R*-HDHA and 10-epi-PDX, obtained from the conversion of DHA and 10*R*-HDHA by *P. homomalla* 8*R*-LOX and *A. violaceum* 15*S*-LOX, respectively, were purified using a preparative HPLC system as described previously (Kim et

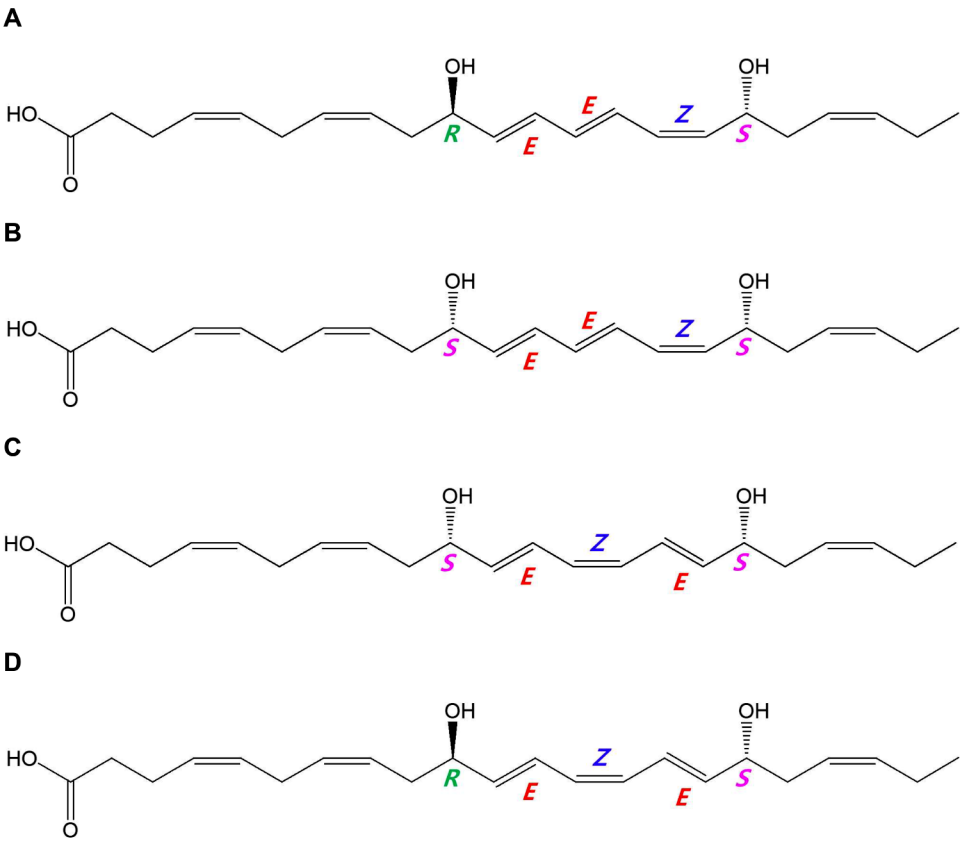

Fig. 1 Chemical structures of 10,17-DiHDHAs (protectins) with different stereoselectivity and *E*-*Z* isomerism. **A** Chemical structure of PD1 (10*R*,17*S*-12*E*,13*E*,15*Z*-triene). **B** Chemical structure of 10-epi PD1 (10*S*,17*S*-12*E*,13*E*,15*Z*-triene). **C** Chemical structure of PDX (10*S*,17*S*-12*E*,13*Z*,15*E*-triene). **D** Chemical structure of 10-epi-PDX (10*R*,17*S*-12*E*,13*Z*,15*E*-triene). 10*R*,17*S*-4*Z*,7*Z*,11*E*,13*Z*,15*E*,19*Z*-DiHDHA was named as 10-epi-PDX

al. 2021; Lee et al. 2020; Oh et al. 2022; Shin et al. 2022). The purified 10*R*-HDHA was used as both a standard and substrate to produce 10-epi-PDX, and the purified 10-epi-PDX was used as a standard.

Microorganisms, plasmid, and gene cloning

E. coli C2566 and pET-28a(+) plasmid were used as the host cells and expression vector, respectively. The gene encoding allene oxide synthase domain-removed 8*R*-LOX from *P. homomalla* (GenBank accession number, AF003692) (Boutaud and Brash 1999; Brash et al. 1996) was synthesized by Bioneer (Daejeon, Republic of Korea). The gene cloning of 15*S*-LOXs (GenBank accession numbers, WP_043395727 and YP_442874) from *A. violaceum* and *Burkholderia thailandensis* was performed as previously described (An et al. 2015; Lee et al. 2020). *Fusarium oxysporum* KACC 40,043 (Korean Agricultural Culture Collection, Jeonju, Republic of Korea) and *Nocardia seiolae* DSM 44,129 (Leibniz Institute DSMZ, Berlin, Germany) were used as the sources of genomic DNA. The genes encoding 15*S*-LOXs (GenBank accession numbers, JH717840 and CP017839) from *F. oxysporum* and *N. seiolae* were cloned using the one-step assembly method. Each 15*S*-LOX gene was ligated into the plasmid pET-28a(+). The ligated plasmid was transformed into *E. coli* C2566.

Culture conditions

A colony of *E. coli* C2566 expressing 8*R*-LOX or 15*S*-LOX was inoculated into 5 mL of Luria – Bertani (LB) medium and cultivated at 37 °C with shaking at 200 rpm overnight. This seed was transferred into a 2 L-Erlenmeyer flask containing 500 mL of LB medium supplemented with 20 mg/mL kanamycin and cultivated at 37 °C with shaking at 200 rpm. As the optical density of culture suspension at 600 nm was 0.8, the enzyme expression induction was started by adding 0.1 mM isopropyl-β-D-thiogalactopyranoside. The culture was further grown for 16 h at 16 °C with shaking at 150 rpm.

Determination of specific activity

The specific activities of *E. coli* cells expressing 8*R*-LOX from *P. homomalla* and 15*S*-LOXs from *(A) violaceum*, *(B) thailandensis*, *F. oxysporum*, and *N. seiolae* towards DHA or HDHA were determined after the reactions were performed in 50 mM HEPES (pH 8.0) containing 2.0 g/L cells, 0.5 mM DHA as a substrate, 200 mM cysteine as a reducing agent, and 5% (v/v) ethanol at 30 °C for 5 min, and in 50

mM CHES buffers (pH 8.5) containing 0.5 g/L cells, 0.5 mM HDHA as a substrate, 200 mM cysteine, and 5% (v/v) ethanol at 20 °C for 5 min. Ethanol at 5% (v/v) was added to the reaction solution to improve compound solubility. The specific activity of the cells was defined as the increase in the amount of product (HDHA or DiHDHA) per unit of dry cell weight (DCW) per unit of reaction time. The cell mass was determined by using a calibration curve relating optical density at 600 nm and DCW, which was determined after the culture broth was centrifuged at 6,000 × *g*, washed with distilled water and dried at 121 °C overnight to a constant weight.

Effects of temperature and pH

The effects of temperature on the conversion of DHA into 10*R*-HDHA and that of 10*R*-HDHA into 10-epi-PDX by *E. coli* expressing *P. homomalla* 8*R*-LOX and *E. coli* expressing *A. violaceum* 15*S*-LOX were investigated at the constant pH values of 8.0 and 8.5 by varying the temperature from 20 to 40 °C in 50 mM HEPES buffer (pH 8.0) and varying that from 15 to 35 °C in 50 mM CHES buffer (pH 8.5), respectively. The effects of pH on the conversion of DHA into 10*R*-HDHA and that of 10*R*-HDHA into 10-epi-PDX were evaluated at the constant temperatures of 30 and 20 °C by varying the pH in the range of 7.0 to 9.0 using 50 mM HEPES (pH 7.0 – 8.0), HEPPS (pH 8.0 – 8.5), and CHES (pH 8.5 – 9.0) buffers and varying that of 7.5 to 9.5 using 50 mM HEPPS (pH 7.5 – 8.5) and CHES (pH 8.5 – 9.5) buffers, respectively. The reactions to produce 10*R*-HDHA and 10-epi-PDX from DHA and 10*R*-HDHA were performed with 0.5 mM of DHA and 10*R*-HDHA, 2.0 and 0.5 g/L cells, 200 mM cysteine, and 5% (v/v) ethanol for 5 min, respectively.

Effects of substrate and cell concentrations

To determine the optimal substrate concentration for maximal production of 10*R*-HDHA, the reactions were performed at 30 ℃ in 50 mM HEPES (pH 8.0) containing 2.0 g/L cells, 200 mM cysteine, and 5% (v/v) ethanol by varying the concentration of DHA from 0.2 to 6.0 mM for 40 min. The optimal cell concentrations for the maximal production of 10*R*-HDHA and 10-epi-PDX were determined at 30 °C using 50 mM HEPES (pH 8.0) and 20 °C using 50 mM CHES (pH 8.5) by varying the cell concentration from 0.25 to 8 g/L with 2.0 mM DHA and varying that from 0.2 to 1.2 g/L with 1.4 mM 10*R*-HDHA, respectively.

Biotransformation of DHA into 10-epi-PDX via 10R-HDHA

The conversion of DHA into 10*R*-HDHA and that of 10*R*-HDHA into 10-epi-PDX by *E. coli* expressing *P. homomalla* 8*R*-LOX and *E. coli* expressing *A. violaceum* 15*S*-LOX were performed at 30 and 20 °C in 50 mM HEPES (pH 8.0) and 50 mM CHES (pH 8.5) containing 4.0 and 1.0 g/L cells, 2.0 mM DHA and 1.4 mM 10*R*-HDHA, 200 mM cysteine, and 5% (v/v) ethanol in a 500 mL-baffled flask containing 100 mL reaction volume for 70 and 50 min, respectively. HEPPS buffer in the serial whole-cell reactions was used without buffer change because the conversion of 10*R*-HDHA into 10-epi-PDX using 50 mM CHES (pH 8.5) was almost the same as that using 50 mM HEPPS (pH 8.5). In the reactions, *E. coli* expressing 8*R*-LOX from *P. homomalla* converted DHA into 10*R*-HDHA using HEPPS buffer (pH 8.0) as described above. After 40 min, the reaction suspension was centrifuged at 3,000 × g for 30 min at 4 °C and cells were then removed using a 0.45 μm nitrocellulose filter membrane (Advantec, Tokyo, Japan). The pH of the filtrate containing 1.4 mM 10*R*-HDHA and 0.6 mM DHA was adjusted to 8.5. The conversion of 10*R*-HDHA into 10-epi-PDX was performed by adding 1.0 g/L of *E. coli* expressing *A. violaceum* 15*S*-LOX to the filtrate and incubating it for additional 50 min under the same conditions as the biotransformation of 10*R*-HDHA into 10-epi-PDX as described above. A control reaction was carried out with untransformed *E. coli* bacterial cells The reaction conditions were the same as those of the experiments with transformed *E. coli*.

HPLC analysis

After the reactions, the solutions were extracted with a double volume of ethyl acetate, which was then removed from the extract and dried using a rotary evaporator, and an equal volume of methanol was added to the dried residue. The concentrations of DHA, 10*R*-HDHA, 17*S*-HDHA, 16,17-hepoxilin B_5, RvD5, and 10-epi-PDX were determined using an HPLC system (Agilent 1260, Santa Clara, CA, USA) with a UV detector at a wavelength of 202 nm and a reversed-phase Nucleosil C18 column (3.2 × 150 nm, 5 μm particle size; Phenomenex, Torrance, CA, USA). The reversed-phase column was eluted at 30 °C for 30 min at a flow rate of 0.25 mL/min with a gradient of solvent A (acetonitrile/water/acetic acid, 50:50:0.1, v/v/v) for 5 min, solvent A to solvent B (acetonitrile/acetic acid, 100:0.1, v/v) for 5–21 min; solvent B for 21–27 min; solvent B to solvent A for 27–32 min; and solvent A for 32–35 min. The chirality of 10-HDHA was analyzed using a chiral-phase Lux Amylose-1 column (6 × 250 mm, 5 μm particle size; Phenomenex) at 234 nm.

The chiral-phase column was eluted at 25 °C with solvent mixtures of *n*-hexane, isopropyl alcohol, and acetic acid (92:8:0.1, v/v/v) at a flow rate of 1.0 mL/min for 35 min. PDX and 10-epi-PDX were also analyzed at 270 nm using a normal-phase Zorbax Rx-sil column (2.1 × 150 mm, 5 µm particle size; Agilent, Santa Clara, CA, USA) for the peak separation of the epimers. The normal-phase columns were eluted at 25 °C with solvent mixtures of *n*-hexane, diethyl ether, and acetic acid (70:30:0.25, v/v/v) at a flow rate of 0.2 mL/min for 35 min.

LC-MS/MS analysis

LC-MS/MS analysis of 10*R*-HDHA and 10-epi-PDX was performed using a Thermo-Finnigan LCQ Deca XP plus ion trap MS (Thermo Fisher Scientific, Waltham, MA, USA) at the National Instrumentation Center for Environmental Management of Seoul National University (Seoul, Republic of Korea). Sample ionization was carried out by electrospray ionization in the negative mode at 275 °C capillary temperature, 5 kV ion source voltage, 207 kPa nebulizer gas, 15 V capillary voltage in negative ionization mode, 46 V capillary voltage in positive mode, 0.6 s average scan time, 1.2 s average time to change polarity, and 35% abundance of precursor ions at collision energy.

Table 1 Specific activities of *E. coli* expressing 8*R*- and *E. coli* expressing 15*S*-LOX towards DHA or HDHA

Substrate	Product	E. coli expressing LOX	Specific activity (mmol/min/mg-cells)
DHA	10*R*-HDHA	*P. homomalla* 8*R*-LOX	20 ± 0.2
	17*S*-HDHA	*A. violaceum* 15*S*-LOX	510 ± 2.1
	17*S*-HDHA	*B. thailandensis* 15*S*-LOX	243 ± 1.7
	17*S*-HDHA	*F. oxysporum* 15*S*-LOX	168 ± 1.4
	17*S*-HDHA	*N. seriolae* 15*S*-LOX	209 ± 1.1
17*S*-HDHA		*P. homomalla* 8*R*-LOX	ND[a]
10*R*-HDHA	10-epi-PDX	*A. violaceum* 15*S*-LOX	280 ± 1.3
	10-epi-PDX	*B. thailandensis* 15*S*-LOX	132 ± 0.9
	10-epi-PDX	*F. oxysporum* 15*S*-LOX	58 ± 0.2
	10-epi-PDX	*N. seriolae* 15*S*-LOX	106 ± 0.5

[a]ND: Not detected

NMR analysis

The chemical structure of 10-epi-PDX was confirmed by recording 1D (^{1}H, ^{13}C, and ^{1}H homo decoupling) and 2D (correlation spectroscopy, rotating frame overhauser enhancement spectroscopy, heteronuclear single quantum coherence, and heteronuclear multiple bond coherence) NMR spectra using an 850 MHz Bruker Avance III HD (Karlsruhe, Germany) equipped with a triple-resonance inverse cryoprobe at the National Center for Inter-University Research Facilities of Seoul National University (Seoul, Republic of Korea). Deuterated methanol was used as both a solvent and an internal standard. All chemical shifts are shown in δ (ppm).

Results

Biosynthetic pathway from DHA to 10-epi-PDX via 10*R*-HDHA by serial reactions of 8*S*- and 15*S*-LOXs

10-Epi-PDX (10*R*,17*S*-12*E*,13*Z*,15*E*-triene) can be produced from DHA via two intermediates 10*R*- and 17*S*-HDHAs by combined reactions of ARA 8*R*- and 15*S*-LOXs. *P. homomalla* 8*R*-LOX was selected and used to produce 10-epi-PDX from DHA via 17*S*-HDHA and 10*R*-HDHA with 15*S*-LOX because the enzyme is the only reported 8*R*-LOX. *P. homomalla* 8*R*-LOX was confirmed to be a soluble protein and was transformed into *E. coli*. *E. coli* expressing *P. homomalla* 8*R*-LOX showed activity for DHA but not for 17*S*-HDHA (Table 1), indicating that *P. homomalla* 8*R*-LOX using DHA was only available for 10*R*-HDHA production. Thus, the enzyme was first used to convert DHA into 10*R*-hydroperoxy-DHA, which was then reduced to 10*R*-HDHA in the presence of a reducing agent such as cysteine (Fig. 2). As the control reaction, untransformed *E. coli* did not convert DHA and 17*S*-HDHA under the same reaction conditions. The formed 10*R*-HDHA was sequentially converted into 10-epi-PDX (10*R*,17*S*-DiHDHA) via 10*R*-hydroxy-17*S*-hydroperoxy-DHA by *A. violaceum* 15*S*-LOX in the presence of the reducing agent.

Selection of 15*S*-LOX for the efficient biotransformation of 10*R*-HDHA into 10-epi-PDX

The putative LOXs from *F. oxysporum* and *N. seiolae* were identified as ARA 15*S*-LOX by characterizing their ARA-derived reaction product as 15*S*-hydroxyeicosatetraenoic acid (data not shown). The specific activities of *E. coli* expressing 15*S*-LOXs from *(A) violaceum*, *(B) thailandensis*, *F. oxysporum*, and *N. seiolae* towards 10*R*-HDHA were compared for their efficiency in the biotransformation

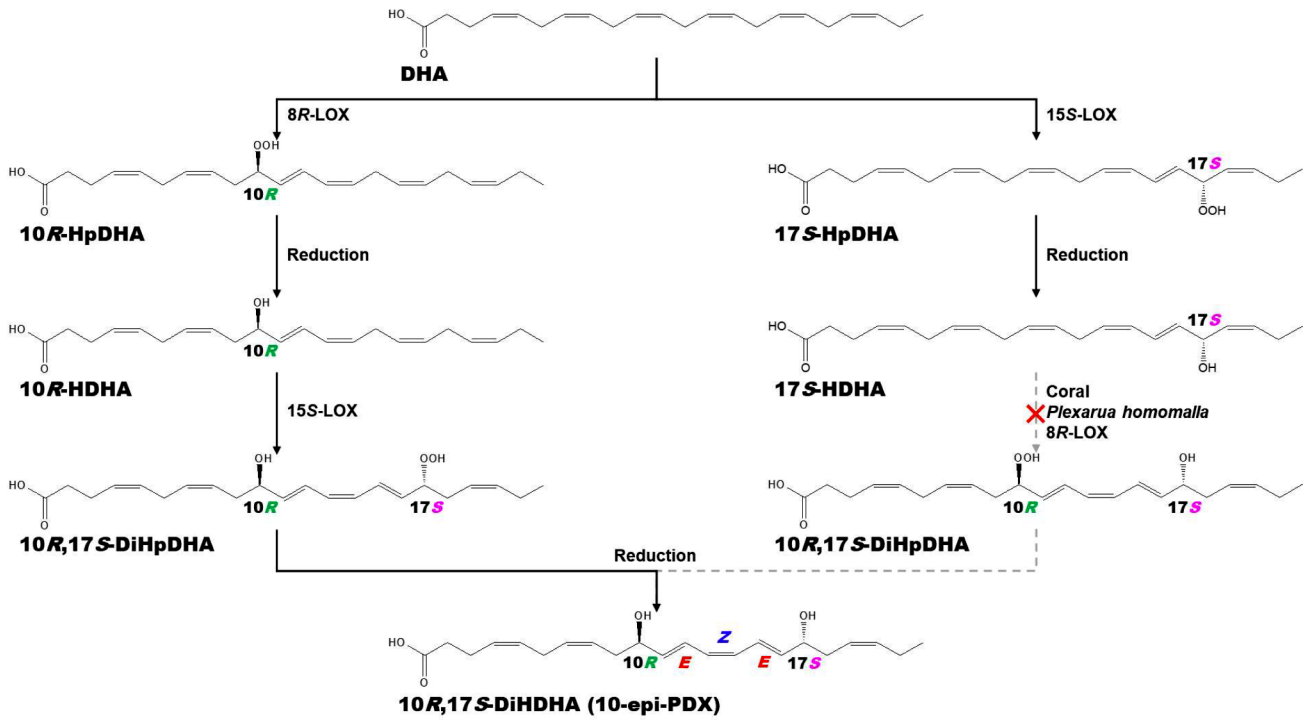

Fig. 2 Biosynthetic pathway from DHA to 10*R*,17*S*-DiHDHA (10-epi-PDX) via 10*R*-HDHA in the presence of cysteine as a reducing agent by the serial reactions of *P. homomalla* 8*R*-LOX and *A. violaceum* 15*S*-LOX. The biosynthetic pathway from DHA to 10-epi-PDX via 17*S*-HDHA is not available because *E. coli* expressing *P. homomalla* 8*R*-LOX shows no activity for 17*S*-HDHA. HpDHA: hydroperoxydocosahexaenoic acid, DiHpDHA: dihydroperoxydocosahexaenoic acid

of 10*R*-HDHA into 10-epi-PDX. The specific activities followed the order *E. coli* expressing *A. violaceum* 15*S*-LOX > *B. thailandensis* 15*S*-LOX > *N. seiolae* 15*S*-LOX > *F. oxysporum* 15*S*-LOX (Table 1). *A. violaceum* 15*S*-LOX, which showed the highest specific activity, was confirmed to be a soluble protein, and *E. coli* expressing it was selected as a biocatalyst, and 10*R*-HDHA, obtained after reacting *E. coli* expressing *P. homomalla* 8*R*-LOX with DHA, was used to produce 10-epi-PDX. As the control reaction, untransformed *E. coli* did not convert 10*R*-HDHA under the same reaction conditions.

Identification of the products obtained from the conversion of DHA and 10*R*-HDHA by *P. Homomalla* 8*R*-LOX and *A. violaceum* 15*S*-LOX

The product obtained from the conversion of DHA by *P. homomalla* 8*R*-LOX was identified as 10*R*-HDHA by comparing the retention time with that of the 10-HDHA standard using HPLC with reversed-phase column (Figure S1) and the 10*S*-HDHA standard and 10(±)-HDHA with chiral-phase column (Fig. 3A). The total molecular mass of the product was indicated by the peak at mass per charge (*m*/*z*) value of 343.8 $[M-H]^-$ in the LC-MS spectrum (Figure S2A), which was the same as that of 10-HDHA (MW = 344.5) with a difference of *m*/*z* 0.3. The critical peaks at *m*/*z* 161.2 and 325.3 in the LC-MS/MS spectrum of the compound (Fig. 4A) were the same as those originating from cleavage between C10 and C11 near the hydroxyl group and the loss of H_2O from the total molecular mass of 10-HDHA with differences of *m*/*z* 0.2, respectively.

The product obtained from the conversion of 10*R*-HDHA by *A. violaceum* 15*S*-LOX was identified as 10,17-DiHDHA by comparing the retention time with that of the 10,17-DiHDHA standard using HPLC with reversed-phase column (Figure S3) In HPLC with normal-phase column, the retention times of the product 10,17-DiHDHA and PDX (10*S*,17*S*-DiHDHA) were different (Fig. 3B). 15*S*-LOX converted 10*S*-HDHA into PDX (10*S*,17*S*-DiHDHA) (Shin et al. 2022), indicating that the product obtained from the conversion of 10*R*-HDHA by *A. violaceum* 15*S*-LOX was 10-epi-PDX (10*R*,17*S*-DiHDHA). Thus, the difference of the retention times was due to the different *R*- and *S*-forms at C10. The retention times of PDX and 10-epi-PDX also differed in the LC/MS chromatograms (Serhan et al. 2006).

In the LC-MS spectrum, the peak at *m*/*z* 359.8 indicated the total molecular mass of the product, corresponding to that of DiHDHA (MW = 360.5) with a difference of *m*/*z* 0.3 (Figure S2B). The fragment peaks at *m*/*z* 153.1, 177.1, and 261.2 in the LC-MS/MS spectrum of the product resulted from cleavages between C9 and C10, C10 and C11, and C16 and C17 near the hydroxyl groups with differences

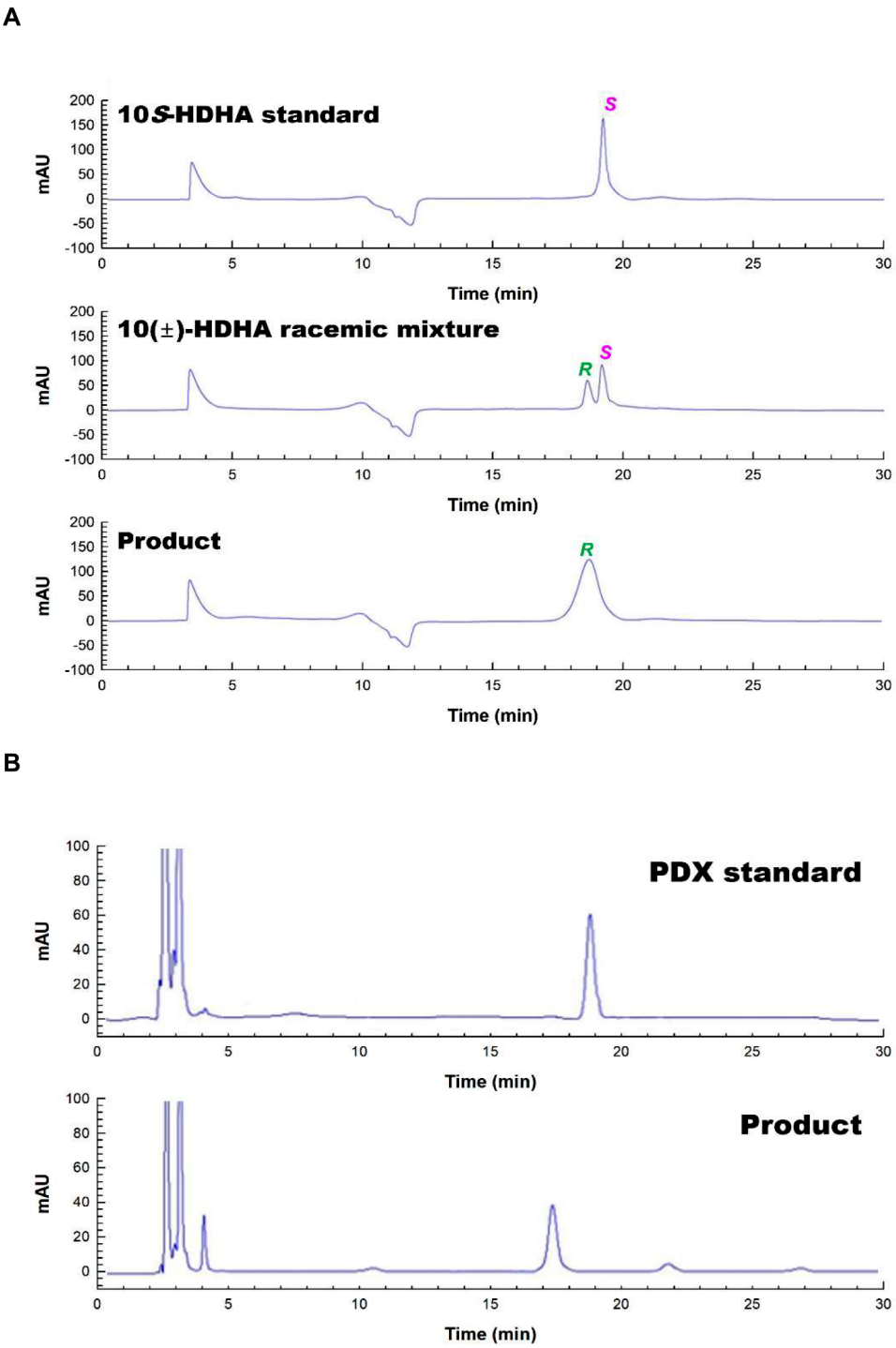

Fig. 3 HPLC chromatograms of the products obtained from the conversion of DHA and 10*R*-HDHA by *P. homomalla* 8*R*-LOX. **A** HPLC chromatograms with chiral-phase column of 10*S*-HDHA standard, 10(±)-HDHA, and the product obtained from the conversion of DHA in the presence of cysteine by *P. homomalla* 8*R*-LOX. **B** HPLC chromatograms with normal-phase column of PDX standard and the product obtained from the conversion of 10*R*-HDHA by *A. violaceum* 15*S*-LOX

within *m*/*z* 0.2, respectively (Fig. 4B). The fragment peak at *m*/*z* 341.3 in the LC-MS/MS spectrum was formed by the loss of H_2O from the total molecular mass with a difference of *m*/*z* 0.2. These results indicate that the product is 10,17-DiHDHA.

The chemical structure of the product obtained from the conversion of 10*R*-HDHA by *A. violaceum* 15*S*-LOX was determined as 10,17-DiHDHA by 1D and 2D NMR analysis (Table S1 and Figure S4). The coupling constants J_{11-12} and J_{15-16} were 15.1 Hz, whereas J_{13-14} was 10.0 Hz. The results indicate that the double bonds of C11 – 12 and C15 – 16 have *E* geometry, whereas that of C13 – 14 has *Z* geometry. The resonance frequencies of two double bonds of H11 – 12 and H15 – 16 were 5.68 – 5.70 and 6.68 – 6.69 ppm, whereas those of three double bonds of H4 – 5, H7 – 8, and H19 – 20 were 5.30 – 5.46 ppm.

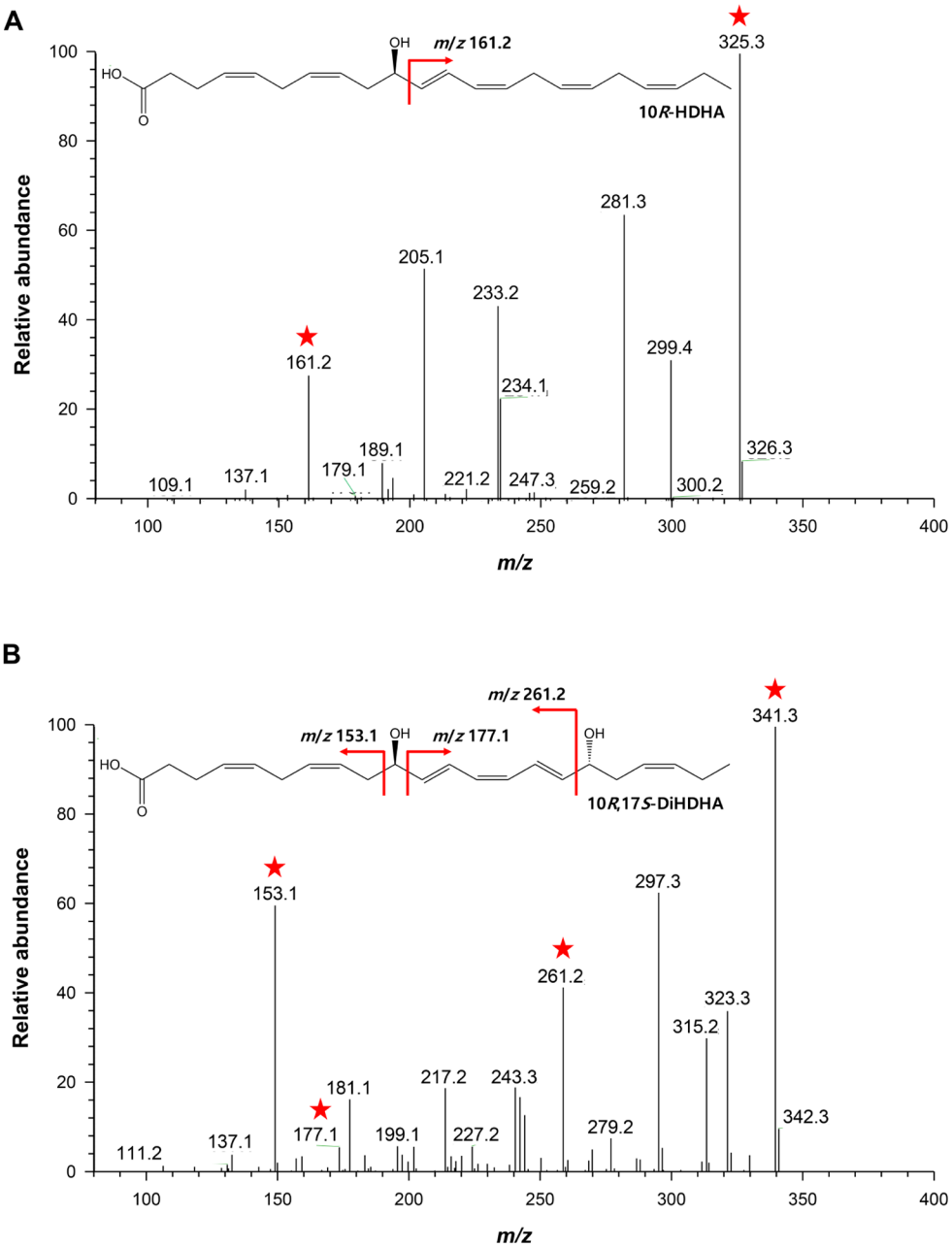

Fig. 4 LC-MS/MS chromatograms of 10*R*-HDHA and 10*R*,17*S*-DiHDHA (10-epi-PDX) obtained from the conversion of DHA and 10*R*-HDHA by *P. homomalla* 8*R*-LOX and *A. violaceum* 15*S*-LOX, respectively. **A** LC-MS/MS chromatogram of 10*R*-HDHA. **B** LC-MS/MS chromatogram of 10*R*,17*S*-DiHDHA (10-epi-PDX). The red-colored star marks indicate critical fragments

The results indicate that the double bonds of C11 – C12 and C15 – C16 have *E* geometry, whereas those of C4 – 5, C7 – 8, and C19 – 20 have *Z* geometry. Thus, the product is 10*R*,17*S*-4*Z*,7*Z*,11*E*,13*Z*,15*E*,19*Z*-DiHDHA.

Biotransformation of DHA into 10*R*-HDHA by *E. Coli* expressing *P. Homomalla* 8*R*-LOX

The effects of temperature and pH on the conversion of DHA as a substrate into 10*R*-HDHA were investigated by *E. coli* expressing *P. homomalla* 8*R*-LOX. The maximal activity was observed at 30 °C and pH 8.0 as an optimal temperature and pH, respectively (Figure S5). The effects of the concentration of DHA and cells on 10*R*-HDHA production was examined, and the maximal production was observed at 2.0 mM DHA and 4.0 g/L cells (Figure S6).

The optimal reaction conditions for 10*R*-HDHA production from DHA by *E. coli* expressing *P. homomalla* 8*R*-LOX were 30 °C, pH 8.0, 2.0 mM DHA, 4.0 g/L cells, and 5% (v/v) ethanol in the presence of 200 mM cysteine. Under these conditions, the cells produced 1.4 mM (482 mg/L) 10*R*-HDHA from (657 mg/L) 2.0 mM DHA for 40 min (Fig. 5A), with a molar conversion of 70%, specific productivity of 8.8 µmol/min/g-cells, and volumetric productivity of 2.1 mM/h.

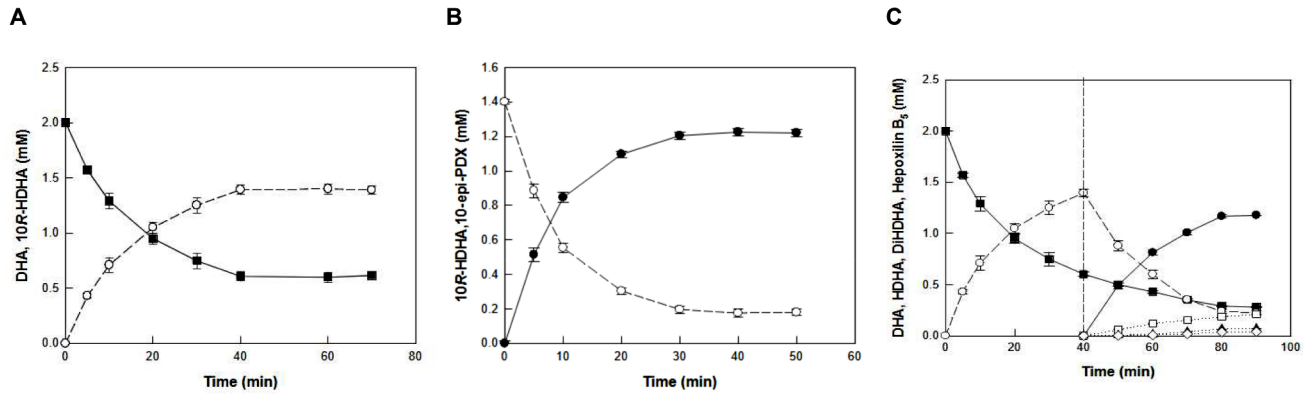

Fig. 5 Time-course biotransformation of DHA into 10-epi-PDX via 10*R*-HDHA. **A** Time-course biotransformation of DHA into 10*R*-HDHA by *E. coli* expressing *P. homomalla* 8*R*-LOX. **B** Time-course biotransformation of 10*R*-HDHA into 10-epi-PDX by *E. coli* expressing *A. violaceum* 15*S*-LOX. The purified 10*R*-HDHA obtained from the conversion of DHA by *E. coli* expressing *P. homomalla* 8*R*-LOX was used as a substrate. **C** Time-course biotransformation of DHA into 10-epi-PDX via 10*R*-HDHA by the serial reactions of *E. coli* expressing *P. homomalla* 8*R*-LOX and *E. coli* expressing *A. violaceum* 15*S*-LOX. *E. coli* expressing *P. homomalla* 8*R*-LOX converted DHA into 10*R*-HDHA. The formed 10*R*-HDHA (open circle) and residual DHA (filled square) were converted into 10-epi-PDX (filled circle); and 17*S*-HDHA (open square), RvD5 (filled triangle), and 16,17-hepoxilin B_5 (open diamond) by *E. coli* expressing *A. violaceum* 15*S*-LOX, respectively. Error bars and data points indicate the standard deviation and means of three experiments, respectively

Biotransformation of 10*R*-HDHA into 10-epi-PDX by *E. Coli* expressing *A. Violaceum* 15*S*-LOX

The effects of temperature and pH on the conversion of 10*R*-HDHA into 10-epi-PDX were examined by *E. coli* expressing *A. violaceum* 15*S*-LOX. The maximal activity was observed at 20 °C and pH 8.5 as an optimal temperature and pH, respectively (Figure S7). The optimal cell concentration for 10-epi-PDX production by *E. coli* expressing *A. violaceum* 15*S*-LOX with 1.4 mM 10*R*-HDHA was investigated (Figure S8). 10-Epi-PDX production was increased with increasing cell concentration up to 1.0 g/L and reached a plateau above this cell concentration. Therefore, the optimal cell concentration for the maximal production of 10-epi-PDX was determined to be 1.0 g/L.

10*R*-HDHA obtained from the conversion of DHA by *E. coli* expressing *P. homomalla* 8*R*-LOX was purified, and the purified 10*R*-HDHA was used as a substrate to biosynthesize 10-epi-PDX. The optimal reaction conditions for the production of 10-epi-PDX from 10*R*-HDHA by *E. coli* expressing *A. violaceum* 15*S*-LOX were 20 °C, pH 8.5, 1.4 mM 10*R*-HDHA, 1.0 g/L cells, and 5% (v/v) ethanol in the presence of 200 mM cysteine. Under these conditions, *E. coli* expressing *A. violaceum* 15*S*-LOX converted 1.4 mM (482 mg/L) 10*R*-HDHA into 1.2 mM (433 mg/L) 10-epi-PDX in 30 min (Fig. 5B), with a molar conversion of 86%, specific productivity of 30.0 µmol/min/g-cells, and volumetric productivity of 2.4 mM/h (865 mg/L/h).

Biotransformation of DHA into 10-epi-PDX via 10*R*-HDHA by serial reactions of *E. Coli* expressing *P. Homomalla* 8*R*-LOX and *E. Coli* expressing *A. Violaceum* 15*S*-LOX

Under each optimal conditions, the serial reactions of *E. coli* expressing *P. homomalla* 8*R*-LOX and *E. coli* expressing *A. violaceum* 15*S*-LOX were performed for 90 min. DHA at 2.0 mM (657 mg/L) was converted into 1.2 mM (433 mg/L) 10-epi-PDX via 1.4 mM (482 mg/L) 10*R*-HDHA in 80 min (Fig. 5C), with a molar conversion of 60% and volumetric productivity of 0.9 mM/h (319 mg/L/h). In the serial reactions, *E. coli* expressing *P. homomalla* 8*R*-LOX converted 2.0 mM DHA into 1.4 mM 10*R*-HDHA in 40 min, with a molar conversion of 70% and volumetric productivity of 2.1 mM/h. After 40 min, *E. coli* expressing *P. homomalla* 8*R*-LOX was removed and 1 g/L of *E. coli* expressing *A. violaceum* 15*S*-LOX was added to the cell-removed solution and incubated for additional 50 min. *E. coli* expressing *A. violaceum* 15*S*-LOX converted 1.4 mM 10*R*-HDHA into 1.2 mM 10-epi-PDX for 40 min, with a molar conversion of 86% and volumetric productivity of 1.8 mM/h (649 mg/L/h). The productivities of 10-epi-PDX in the serial reactions were 1.3-fold lower than those using 1.4 mM purified 10*R*-HDHA due to the presence of DHA. The residual DHA derived from the first whole-cell reaction was converted into byproducts, including 0.21 mM 17*S*-HDHA, 0.07 mM RvD5, and 0.04 mM 16,17-hepoxilin B_5, by *E. coli* expressing *A. violaceum* 15*S*-LOX.

Discussion

The biosynthetic pathways from DHA to PD1 and PDX are constructed by utilizing different mechanisms of 15*S*-LOX (An et al. 2021; Stenvik Haatveit and Hansen 2023). The epoxidation activity of 15*S*-LOX converts DHA into the intermediate 16*S*,17*S*-epoxy-DHA, which is hydrolyzed to PD1 (10*R*,17*S*-11*E*,13*E*,15*Z*-triene) by epoxide hydrolase (Aursnes et al. 2015), whereas the oxygenation activity of 15*S*-LOX converts DHA into the intermediate 17*S*-HDHA under reduction conditions, which is converted into PDX (10*S*,17*S*-11*E*,13*Z*,15*E*-triene) by its double oxygenation activity (Serhan et al. 2015b) or by 8*S*-LOX (Shin et al. 2022) (Figure S9). Owing to the different mechanism, PDX shows a different stereoselectivity at C10 with a different *E*-*Z* isomerism of double bonds to that of PD1. 10-Epi-PDX shows the same *E*-*Z* isomerism compared to that of PDX because the mechanism is same. However, it exhibits a different stereoselectivity at C10 because a different stereoselective LOX is used.

The chirality of the product obtained from the conversion of DHA by *P. homomalla* 8*R*-LOX was *R*-form by HPLC analysis with chiral-phase column (Fig. 3A). The chirality at C10 of the DiHDHA product obtained from the conversion of 10*R*-HDHA by *A. violaceum* 15*S*-LOX was *R*-form because it derived from 10*R*-HDHA. In HPLC profiles, the retention times of the products 10,17-DiHDHA and PDX (10*S*,17*S*-DiHDHA) were different (Fig. 3B). The product obtained from the conversion of DHA by the serial reactions of 8*R*- and 15*S*-LOXs was 10*R*,17*S*-DiHDHA because PDX (10*S*,17*S*-DiHDHA) was produced by the serial reactions of 8*S*- and 15*S*-LOXs (Shin et al. 2022). The *E*-*Z* geometry of double bonds of the product by NMR analysis was 4*Z*,7*Z*,11*E*,13*Z*,15*E*,19*Z* (Table S1 and Figure S4). Thus, the product was identified as 10*R*,17*S*-4*Z*,7*Z*,11*E*,13*Z*,15*E*,19*Z*-DiHDHA. The C10 epimer form of PD1 (10*R*,17*S*-4*Z*,7*Z*,11*E*,13*E*,15*Z*,19*Z*-DiHDHA) has been called 10-epi PD1 (10*S*,17*S*-4*Z*,7*Z*,11*E*,13*E*,15*Z*,19*Z*-DiHDHA) with different stereoselectivity of the hydroxyl group at C10 and the same *E*-*Z* geometry of double bonds (An et al. 2021; Balas and Durand 2016). The product (10*R*,17*S*-4*Z*,7*Z*,11*E*,13*Z*,15*E*,19*Z*-DiHDHA) is named 10-epi-PDX because it is the C10 epimer form of PDX (10*S*,17*S*-4*Z*,7*Z*,11*E*,13*Z*,15*E*,19*Z*-DiHDHA) (Fig. 1). The two diastereomers, 10-epi-PDX and PDX (Shin et al. 2022), have different electronic structures with distinguishable NMR spectroscopy due to the different stereoselectivity at C10 (Figure S10).

In the biotransformation reactions, the extracellular reducing agent was essential to reduce the formed hydroperoxy fatty acids during the reactions to hydroxy fatty acids because the hydroperoxy fatty acids were present in the product and the activities of endogenous bacterial peroxidases were not enough to reduce the formed hydroperoxy fatty acids during the short reaction time within 90 min. We used cysteine as a reducing agent in the present study because it reduced completely the formed hydroperoxy fatty acids to hydroxy fatty acids. For more efficient reduction, the choosing test of much stronger reducing agent is required.

As the control reaction, untransformed *E. coli* did not convert DHA, whereas *E. coli* expressing *P. homomalla* 8*R*-LOX converted DHA to 10*R*-HDHA. The only one reported 8*R*-LOX *P. homomalla* 8*R*-LOX was used, and the expression of 8*R*-LOX was confirmed as soluble protein (Brash et al. 1996). *E. coli* expressing *P. homomalla* 8*R*-LOX converted the substrate DHA into 10*R*-HDHA, whereas *E. coli* expressing mouse 8*S*-LOX converted DHA in DHA-enriched fish oil hydrolyzate (DFOH) into 10*S*-HDHA (Shin et al. 2022). The composition of DFOH is not the same as the reagent-grade DHA (99%). DFOH contains not only DHA, but also DPA, EPA, ARA, other fatty acids, and glycerol because it is obtained from DHA-enriched fish oil by hydrolysis of fish oil. However, the reagent-grade DHA contains no or little these by-products. Other by-products besides DHA of DFOH and other hydroxy fatty acids produced from other fatty acids by 8*S*-LOX might inhibit the enzyme reaction. Therefore, the comparison was not exact because different substrates were used. Nevertheless, the production of 10*R*-HDHA was compared to that of 10*S*-HDHA (Table 2). The product concentration, molar conversion, and specific and volumetric productivities for the biocatalytic synthesis of 10*R*-HDHA from DHA were 3.3-, 1.6-, 24-, and 29-fold higher than those of 10*S*-HDHA from DHA in DFOH, respectively, suggesting that the production of 10*R*-HDHA by *E. coli* expressing *P. homomalla* 8*R*-LOX is more efficient than that of 10*S*-HDHA by *E. coli* expressing mouse 8*S*-LOX.

As the control reaction, untransformed *E. coli* did not convert 10*R*-HDHA, whereas *E. coli* expressing *A. violaceum* 15*S*-LOX converted 10*R*-HDHA to 10-epi-PDX. The expression of *(A) violaceum* 15*S*-LOX was confirmed as soluble protein (Lee et al. 2020). Microbial 15*S*-LOXs have been reported from *A violaceum*, *(B) thailandensis*, *Pseudomonas aeruginosa*, and *Oscillatoria nigro-viridis* (An et al. 2021). We have only 15*S*-LOXs from *A violaceum* and *B. thailandensis*, while those from *F oxysporum* and *N. seiolae* are newly cloned and identified. Therefore, these 15*S*-LOXs are chosen for evaluation. The product concentration, molar conversion, and specific and volumetric productivities for the production of 10-epi-PDX (10*R*,17*S*-DiHDHA) from 10*R*-HDHA by *E. coli* expressing *(A) violaceum* 15*S*-LOX were 4.0-, 1.2-, 143-, and 35-fold higher than those for the production of PDX (10*S*,17*S*-DiHDHA) from 10*S*-HDHA

Table 2 Biotransformation of DHA into 10-epi-PDX (10*R*,17*S*-DiHDHA) or PDX (10*S*,17*S*-DiHDHA) via 10*R*-HDHA or 10*S*-HDHA by serial reactions of *E. coli* expressing 8*S*-LOX or 8*R*-LOX and *E. coli* expressing 15*S*-LOX, respectively

Biocatalyst (LOX expressed in E. coli)	Substrate (mM)	Product (mM)	Specific productivity (μmol/min/g-cells)	Volumetric productivity (μM/h)	Molar conversion (%)	Reference
Mouse 8*S*-LOX	DHA in DFOH[a] (1.0)	10*S*-HDHA (0.43)	0.36 ± 0.01	72 ± 2.0	43.0 ± 1.0	(Shin et al. 2022)
B. thailandensis 15*S*-LOX	10*S*-HDHA in mouse 8*S*-LOX treated DFOH (0.43)	10*S*,17*S*-DiHDHA (0.30)	0.21 ± 0.01	60 ± 1.0	69.8 ± 2.3	(Shin et al. 2022)
Mouse 8*S*-LOX + 15*S*-LOX *B. thailandensis*	DHA in DFOH (1.0)	10*S*,17*S*-DiHDHA (0.30)		25 ± 0.5	30.0 ± 0.1	(Shin et al. 2022)
P. homomalla 8*R*-LOX	DHA (2.0)	10*R*-HDHA (1.4)	8.8 ± 0.2	2,100 ± 68	70.0 ± 2.3	This study
A. violaceum 15*S*-LOX	10*R*-HDHA (1.4)	10*R*,17*S*-DiHDHA (1.2)	30.0 ± 0.5	2,400 ± 27	85.7 ± 1.3	This study
P. homomalla 8*R*-LOX + *A. violaceum* 15*S*-LOX	DHA (2.0)	10*R*,17*S*-DiHDHA (1.2)		886 ± 12	58.9 ± 0.5	This study

[a]DFOH, DHA-enriched fish oil hydrolyzate

derived from DFOH by *E. coli* expressing *(B) thailandensis* 15*S*-LOX, respectively (Table 2). The specific activity of *E. coli* expressing *(A) violaceum* 15*S*-LOX towards 10*R*-HDHA was 2.1-fold higher than that of *E. coli* expressing *(B) thailandensis* 15*S*-LOX (Table 1), which was used for the biotransformation of 10*S*-HDHA into PDX (Shin et al. 2022). These results suggest that *E. coli* expressing *(A) violaceum* 15*S*-LOX to produce 10-epi-PDX is a more efficient biocatalyst than *E. coli* expressing *(B) thailandensis* 15*S*-LOX to produce PDX.

DHA in DFOH at 1.0 mM was converted into 0.3 mM PDX via 0.43 mM 10*S*-HDHA by the serial reactions of *E. coli* expressing mouse 8*S*-LOX and *E. coli* expressing *B. thailandensis* 15*S*-LOX in 12 h, with a molar conversion of 30% and volumetric productivity of 25 μM/h (Shin et al. 2022). The product concentration, molar conversion, and volumetric productivity for the production of 10-epi-PDX from DHA were 4.0-, 2.0-, and 31-fold higher than those for the production of PDX from DHA in DFOH, respectively (Table 2). The results suggest that the biocatalyst system for the production of 10-epi-PDX using DHA is superior to that of PDX.

Conclusions

The synthesis of 10-epi-PDX by mammalian cell culture is not viable for providing it for research purposes because they are produced in small amounts. Thus, we performed the quantitative production of 10-epi-PDX from DHA by the serial whole-cell biotransformation of *E. coli* expressing 8*R*-LOX and *E. coli* expressing 15*S*-LOX. In the biotransformation, 433 mg/L (1.2 mM) 10-epi-PDX was obtained from 657 mg/L (2.0 mM) DHA in 80 min, with a conversion of 66% (w/w) and volumetric productivity of 319 mg/L/h. To the best of our knowledge, this is the first quantitative production of 10-epi-PDX. The quantitative production can supply large amounts of 10-epi-PDX for research purposes. Our results will contribute to providing a sufficient supply of 10-epi-PDX to study its efficacy and functionality.

Supplementary Information The online version contains supplementary material available at https://doi.org/10.1007/s11274-024-04032-9.

Acknowledgements This study was supported by the Mid-Career Researcher Program, through the National Research Foundation grant (Grant No. RS-2024-00340835) funded by the Ministry of Science and ICT; and the Korea Institute of Planning and Evaluation for Technology in Food, Agriculture, and Forestry (Grant No. RS-2024-00398879) of the Ministry of Agriculture, Food, and Rural Affairs, Republic of Korea; and Hankuk University of Foreign Studies Research Fund of 2024.

Author contributions T. E. Lee, Y. J. Ko, K. C. Shin, and D. K. Oh wrote the main manuscript text. T. E. Lee, K. C. Shin, and D. K. Oh prepared Figs. 1, 2, 3, 4, 5 and 6; Table 1, and 2. Y. J. Ko prepared NMR data in supplementary information. All authors reviewed the manuscript.

Data availability The data that support the findings of this study are available from the corresponding author upon reasonable request.

Declarations

Ethical approval This article does not contain any studies with human participants or animals performed by any of the authors.

Competing interests The authors declare no competing interests.

Conflict of interest The authors declare no competing financial interest.

References

An JU, Kim BJ, Hong SH, Oh DK (2015) Characterization of an omega-6 linoleate lipoxygenase from *Burkholderia thailandensis* and its application in the production of 13-hydroxyoctadecadienoic acid. Appl Microbiol Biotechnol 99(13):5487–5497. https://doi.org/10.1007/s00253-014-6353-8

An JU, Kim SE, Oh DK (2021) Molecular insights into lipoxygenases for biocatalytic synthesis of diverse lipid mediators. Prog Lipid Res 83. https://doi.org/10.1016/j.plipres.2021.101110

Antony R, Lukiw WJ, Bazan NG (2010) Neuroprotectin D1 induces dephosphorylation of Bcl-x_L in a PP2A-dependent manner during oxidative stress and promotes retinal pigment epithelial cell survival. J Biol Chem 285(24):18301–18308. https://doi.org/10.1074/jbc.M109.095232

Asatryan A, Bazan NG (2017) Molecular mechanisms of signaling via the docosanoid neuroprotectin D1 for cellular homeostasis and neuroprotection. J Biol Chem 292(30):12390–12397. https://doi.org/10.1074/jbc.R117.783076

Aursnes M, Tungen JE, Colas RA, Vlasakov I, Dalli J, Serhan CN, Hansen TV (2015) Synthesis of the 16*S*,17*S*-epoxyprotectin intermediate in the biosynthesis of protectins by human macrophages. J Nat Prod 78(12):2924–2931. https://doi.org/10.1021/acs.jnatprod.5b00574

Balas L, Durand T (2016) Dihydroxylated *E,E,Z*-docosatrienes. An overview of their synthesis and biological significance. Prog Lipid Res 61:1–18. https://doi.org/10.1016/j.plipres.2015.10.002

Borgeson E, Johnson AM, Lee YS, Till A, Syed GH, Ali-Shah ST, Godson C (2015) Lipoxin A4 attenuates obesity-induced adipose inflammation and associated liver and kidney disease. Cell Metab 22(1):125–137. https://doi.org/10.1016/j.cmet.2015.05.003

Boutaud O, Brash AR (1999) Purification and catalytic activities of the two domains of the allene oxide synthase-lipoxygenase fusion protein of the coral *Plexaura homomalla*. J Biol Chem 274(47):33764–33770. https://doi.org/10.1074/jbc.274.47.33764

Brash AR, Boeglin WE, Chang MS, Shieh BH (1996) Purification and molecular cloning of an 8*R*-lipoxygenase from the coral *Plexaura homomalla* reveal the related primary structures of *R*- and *S*-lipoxygenases. J Biol Chem 271(34):20949–20957. https://doi.org/10.1074/jbc.271.34.20949

Chen P, Fenet B, Michaud S, Tomczyk N, Vericel E, Lagarde M, Guichardant M (2009) Full characterization of PDX, a neuroprotectin/protectin D1 isomer, which inhibits blood platelet aggregation. Febs Lett 583(21):3478–3484. https://doi.org/10.1016/j.febslet.2009.10.004

Dayaker G, Durand T, Balas L (2014) A versatile and stereocontrolled total synthesis of dihydroxylated docosatrienes containing a conjugated *E*,*E*,*Z*-triene. Chem-Eur J 20(10):2879–2887. https://doi.org/10.1002/chem.201304526

Gobbetti T, Dalli J, Colas RA, Canova F, Aursnes D, Bonnet M, Perretti D, M (2017) Protectin $D1_{n\text{-}3\ DPA}$ and resolvin $D5_{n\text{-}3\ DPA}$ are effectors of intestinal protection. Proc Natl Acad Sci USA 114(15):3963–3968. https://doi.org/10.1073/pnas.1617290114

Hwang HJ, Jung TW, Kim JW, Kim JA, Lee YB, Hong SH, Yoo HJ (2019) Protectin DX prevents H_2O_2-mediated oxidative stress in vascular endothelial cells via an AMPK-dependent mechanism. Cell Signal 53:14–21. https://doi.org/10.1016/j.cellsig.2018.09.011

Kim TH, Lee J, Kim SE, Oh DK (2021) Biocatalytic synthesis of dihydroxy fatty acids as lipid mediators from polyunsaturated fatty acids by double dioxygenation of the microbial 12*S*-lipoxygenase. Biotechnol Bioeng 118(8):3094–3104. https://doi.org/10.1002/bit.27820

Lagarde M, Guichardant M, Bernoud-Hubac N (2020) Anti-inflammatory and anti-virus potential of poxytrins, especially protectin DX. Biochimie 179:281–284. https://doi.org/10.1016/j.biochi.2020.09.008

Lee IG, An JU, Ko YJ, Park JB, Oh DK (2019) Enzymatic synthesis of new hepoxilins and trioxilins from polyunsaturated fatty acids. Green Chem 21(11):3172–3181. https://doi.org/10.1039/c9gc01031a

Lee J, An JU, Kim TH, Ko YJ, Park JB, Oh DK (2020) Discovery and engineering of a microbial double-oxygenating lipoxygenase for synthesis of dihydroxy fatty acids as specialized proresolving mediators. ACS Sustain Chem Eng 8(43):16172–16183. https://doi.org/10.1021/acssuschemeng.0c04793

Morita M, Kuba K, Ichikawa A, Nakayama M, Katahira J, Iwamoto R, Imai Y (2013) The lipid mediator protectin D1 inhibits influenza virus replication and improves severe influenza. Cell 153(1):112–125. https://doi.org/10.1016/j.cell.2013.02.027

Oh CW, Kim SE, Lee J, Oh DK (2022) Bioconversion of C20- and C22-polyunsaturated fatty acids into 9*S*,15*S*- and 11*S*,17*S*-dihydroxy fatty acids by *Escherichia coli* expressing double-oxygenating 9*S*-lipoxygenase from *Sphingopyxis macrogoltabida*. J Biosci Bioeng 134(1):14–20. https://doi.org/10.1016/j.jbiosc.2022.04.001

Perry SC, Kalyanaraman C, Tourdot BE, Conrad WS, Akinkugbe O, Freedman JC, Holman TR (2020) 15-Lipoxygenase-1 biosynthesis of 7*S*,14*S*-diHDHA implicates 15-lipoxygenase-2 in biosynthesis of resolvin D5. J Lipid Res 61(7):1087–1103. https://doi.org/10.1194/jlr.RA120000777

Rodriguez AR, Spur BW (2005) First total synthesis of 7(*S*),17(*S*)-resolvin D5, a potent anti-inflammatory docosanoid. Tetrahedron Lett 46(21):3623–3627. https://doi.org/10.1016/j.tetlet.2005.03.175

Sanceau JY, Maltais R, Poirier D, Marette A (2019) Total synthesis of the antidiabetic (type 2) lipid mediator protectin DX/PDX. J Org Chem 84(2):495–505. https://doi.org/10.1021/acs.joc.8b01973

Serhan CN, Gotlinger K, Hong S, Lu Y, Siegelman J, Baer T, Petasis NA (2006) Anti-inflammatory actions of neuroprotectin D1/protectin D1 and its natural stereoisomers: assignments of dihydroxy-containing docosatrienes. J Immunol 176(3):1848–1859. https://doi.org/10.4049/jimmunol.176.3.1848

Serhan CN, Yang R, Martinod K, Kasuga K, Pillai PS, Porter TF, Spite M (2009) Maresins: novel macrophage mediators with potent antiinflammatory and proresolving actions. J Exp Med 206(1):15–23. https://doi.org/10.1084/jem.20081880

Serhan CN, Chiang N, Dalli J (2015a) The resolution code of acute inflammation: Novel pro-resolving lipid mediators in resolution. Semin Immunol 27(3):200–215. https://doi.org/10.1016/j.smim.2015.03.004

Serhan CN, Dalli J, Colas RA, Winkler JW, Chiang N (2015b) Protectins and maresins: new pro-resolving families of mediators in acute inflammation and resolution bioactive metabolome. Biochim Biophys Acta 1851(4):397–413. https://doi.org/10.1016/j.bbalip.2014.08.006

Shin KC, Lee TE, Kim SE, Ko YJ, Seo MJ, Oh DK (2022) Enzymatic formation of protectin dx and its production by whole-cell reaction using recombinant lipoxygenases. Catalysts 12(10). https://doi.org/10.3390/catal12101145

Spite M, Norling LV, Summers L, Yang R, Cooper D, Petasis NA, Serhan CN (2009) Resolvin D2 is a potent regulator of leukocytes and controls microbial sepsis. Nature 461(7268):1287–U1125. https://doi.org/10.1038/nature08541

Stenvik Haatveit A, Hansen TV (2023) The biosynthetic pathways of the protectins. Prostaglandins Other Lipid Mediat 169:106787. https://doi.org/10.1016/j.prostaglandins.2023.106787

Tungen JE, Aursnes M, Hansen TV (2015) Stereoselective synthesis of maresin 1. Tetrahedron Lett 56(14):1843–1846. https://doi.org/10.1016/j.tetlet.2015.02.080

Werz O, Gerstmeier J, Libreros S, De la Rosa X, Werner M, Norris PC, Serhan CN (2018) Human macrophages differentially produce specific resolvin or leukotriene signals that depend on bacterial pathogenicity. Nat Commun 9(1):59. https://doi.org/10.1038/s41467-017-02538-5

Weylandt KH (2016) Docosapentaenoic acid derived metabolites and mediators - the new world of lipid mediator medicine in a nutshell. Eur J Pharmacol 785:108–115. https://doi.org/10.1016/j.ejphar.2015.11.002